Summary: A series of polyimide/ZnO nanohybrid films with different ZnO content were prepared from a rigid pyromellitic dianhydride-4,4′-diaminodiphenyl ether (PMDA-ODA) polyimide (PI) and a flexible 3,3′,4,4′-benzophenonetetracarboxylic acid dianhydride-4,4′-diaminodiphenyl ether (BTDA-ODA) PI with ZnO nanoparticles (3–4 nm). Fourier-transform infrared (FT-IR) and X-ray photoelectron spectroscopy (XPS) depict that the ZnO nanoparticles function as a physical cross-linking agent with PI through hydrogen bonding between the OH on the ZnO nanoparticles and the C=O of the imide groups. ZnO nanoparticles in the rigid PMDA-ODA matrix cause a larger percentage decrease in the coefficient of linear thermal expansion (CTE) than in the flexible BTDA-ODA matrix. The BTDA-ODA/ZnO hybrid films have two transition peaks in dynamic mechanical tan δ curves, but PMDA-ODA/ZnO hybrid films only have one transition peak. Thermogravimetric analysis reveals that ZnO decreases the thermal degradation temperature (T_d) in both hybrid films, but less so in PMDA-ODA/ZnO films. Transmission electron microscopy (TEM) images reveal that the rigid matrix induces larger particle size (30–40 nm) compared to the flexible matrix (10–15 nm).

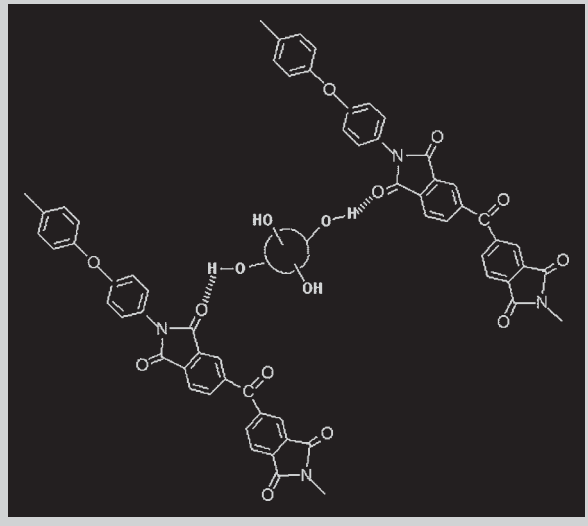

Illustration of the interaction between ZnO nanoparticles and PI.

Effect of the Polyimide Structure and ZnO Concentration on the Morphology and Characteristics of Polyimide/ZnO Nanohybrid Films

Shou-Chian Hsu, Wha-Tzong Whang, Chin-Hsien Hung, Pei-Chun Chiang, Yi-Nan Hsiao*

Institute of Materials Science & Engineering, National Chiao Tung University, 1001 Ta Hsueh Road, Hsin Chu, Taiwan 300, Republic of China
Fax: 886-3-5724727; E-mail: wtwhang@mail.nctu.edu.tw

Received: August 6, 2004; Revised: November 12, 2004; Accepted: November 15, 2004; DOI: 10.1002/macp.200400326

Keywords: nanocomposites; polyimides; structure-property relations; thermal properties; ZnO

Introduction

Metal or semiconductor nanoparticles dispersed in polymeric matrixes have been widely studied recently.[1–5] These nanocomposites exhibit interesting properties and could be widely applied in the microelectronic and optoelectronic industries. Polyimide (PI) is a promising matrix for these nanocomposites because of its good thermal stability and chemical resistance.[5–7] The mechanical, electrical, and optical properties of pure PI are further improved by incorporating inorganic materials.

Zinc oxide (ZnO) has attracted much attention because of its excellent physical properties, such as a wide band gap (3.37 eV) at room temperature and a large exciton bonding energy (60 meV). It can be used in ultraviolet light-emitting diodes, transparent electrodes, and piezoelectric devices etc.[8,9] Many different methods have been reported to fabricate ZnO nanocrystals. Spanhel and Anderson[10] reported a simple sol-gel method to prepare quantum size ZnO particles. To obtain a sharp size distribution, the use of surfactant- or polymer-stabilized ZnO nanoparticles has been reported.[11–13]

Several ZnO/organic composites have been reported, such as poly(ethylene glycol),[14] low density polyethylene,[15] poly(ethylene oxide),[16] Nylon-6, and poly(styrene butyl acrylate).[17] Our laboratory successfully prepared highly

transparent and stable luminescent ZnO/poly(hydroxyethyl methacrylate) nanocomposites.[18] However, the inferior thermal stability of organic matrices may restrict a composite's application in the electronic and optoelectronic industries. For electronic and optoelectronic applications, high reliability usually requires a highly thermal stable polymer matrix. PI is a well-known thermally stable polymer. In this study, we chose two different PIs, 3,3′,4,4′-benzophenonetetracarboxylic acid dianhydride-4,4′-diaminodiphenyl ether (BTDA/ODA) and pyromellitic dianhydride-4,4′-diaminodiphenyl ether (PMDA/ODA), as host polymers to synthesize a series of PI/ZnO nanocomposites with different ZnO content. The first PI is more flexible than the second PI. We intend to study the effect of PI characteristics on the size of ZnO in PI and the characteristics of the PI/ZnO nanohybrid films. First, quantum-dot ZnO nanoparticles with a modified surfactant are prepared. The ZnO is then introduced to the poly(amic acid) PI precursors, and finally, the composite is thermally imidized to form PI/ZnO nanohybrid films. The thermal, mechanical, and morphology characteristics of the hybrid films are investigated to understand the effect of the ZnO content and PI structure on these characteristics. In addition, the effects of polyimide structure on the size of ZnO and the structural variation of ZnO nanoparticles before and after thermal imidization are reported.

Experimental Part

Materials

Zinc acetate dihydrate (99.0%) from Showa, lithium hydroxide monohydrate (99.0%) from TEDIA, 3-(trimethoxysilyl)propyl methacrylate (TPM, 98%) from Aldrich, absolute ethanol (99.5%) and dimethyl sulfoxide (DMSO) from Nasa, 4,4′-diaminodiphenyl ether (ODA, 98%), 3,3′,4,4′-benzophenonetetracarboxylic acid dianhydride (BTDA, 99%), and pyromellitic dianhydride (PMDA, 99%) from TCI, were used as received without further purification.

Synthesis of ZnO-TPM Nanoparticles

ZnO nanoparticle colloids with an average particle size of 3.2 nm were first prepared from zinc acetate dihydrate, lithium hydroxide monohydrate, and absolute ethanol according to the method of Spanhel and Anderson.[10] The ZnO nanoparticles produced were further stabilized by adding TPM. The TPM (molar ration of TPM to ZnO was 1:10) was diluted in 10 mL ethanol, and then added dropwise to the ZnO nanoparticle colloids under continuous stirring. The reaction proceeded for 12 h. The synthetic TPM-stabilized ZnO-nanoparticle solution was filtered through a 0.1 μm glass fiber filter. The nanoparticles were washed with heptane/ethanol several times. Finally, the solvent (ethanol) of the TPM-stabilized ZnO solution was replaced by the same amount of DMSO using rotary evaporation. The details of the synthesis route and characterization of the stabilized ZnO has been reported in our previous research paper.[18]

Preparation of the PI/ZnO Nanocomposites

The procedures for preparing poly(amic acid) and PI/ZnO nanocomposites are shown in Figure 1. The polycondensation was carried out in a flask by adding the diamine ODA (2.002 g, 0.01 mol) and the dianhydride BTDA (3.222 g, 0.01 mmol) in DMSO (30 mL) under a nitrogen stream at room temperature. BTDA was added to the solution in five portions. After the dissolution of all BTDA, the reaction mixture was further

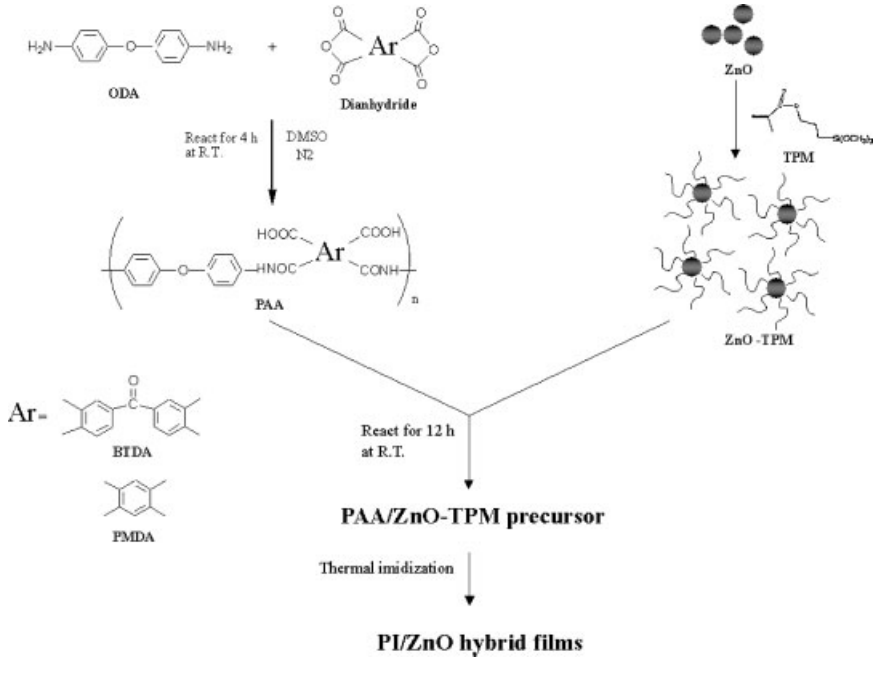

Figure 1. Synthetic route to prepare PI/ZnO hybrid films.

stirred for 2 h at room temperature. Various amounts of the TPM-stabilized ZnO DMSO solution were added dropwise to the PAA solution and further stirred for 12 h. The modified and unmodified PAA solutions were cast on glass plates, and then step-heated at 100, 150, and 200 °C, for 1 h at each temperature, and finally at 300 °C for 2 h. The PI/ZnO nanohybrid films have an average thickness of 30–35 μm. The hybrid films of the PMDA series were prepared in a similar manner.

Measurements

Thermogravimetric analysis (TGA) was used to characterize the thermal stability of the polyimides with a TA Instruments TGA 2950 at a heating rate of 20 °C · min^{-1} from 30–900 °C under nitrogen. The coefficient of the linear thermal expansion (CTE) was measured by thermomechanical analysis (TMA) with a TA Instruments TMA 2940 at heating rate of 10 °C · min^{-1}. The glass transition temperature (T_g) measurement with dynamic mechanical experiments was performed using a DuPont DMA Q800 Dynamic Mechanical Analyzer at 5 °C · min^{-1} and a frequency 1 Hz. Fourier-transform infrared (FT-IR) spectra were measured with a Nicolet Protégé 460. XPS spectra were obtained by using an ESCA PHI 1600 spectrometer working in the constant analyzer energy mode with a pass energy of 50 eV and Mg K_α (1 253.6 eV) radiation as the excitation source. XPS analysis was done at room temperature and pressures below 10^{-10} Torr. The take-off angle used in the XPS measurements was 90°. Transmission electron microscopy (TEM) imaging was performed using a JEOL-200FX transmission electron microscope.

Results and Discussion

Infrared spectra of BTDA/ODA pure PI and BTDA-ODA/ZnO nanocomposites are shown in Figure 2(b)–(e). In Figure 2(c)–(e), all the hybrid films exhibit the characteristic absorption peaks of imide groups at 1 772, 1 719, and 1 380 cm^{-1}. The former two peaks are caused by asymmetric and symmetric C=O stretching and the last peak is associated with the C–N stretching. The intensity of the absorption band at 3 200–3 700 cm^{-1} increased with increasing ZnO content and this may be related to different states of hydrogen bonding. The characteristic imide peaks (C=O) of these hybrid films are shifted towards lower wavenumbers compared to that of the pure PI (Figure 2b). Hydrogen-bond formation between the C=O of the imide group and the OH group in ZnO nanoparticles can account for the phenomenon.[19–21] However, the Si–O–Si or Si–O absorption at 1 200–1 050 cm^{-1} in the TPM-stabilized ZnO nanoparticles (Figure 2a) was also found in the PI/ZnO hybrid films.

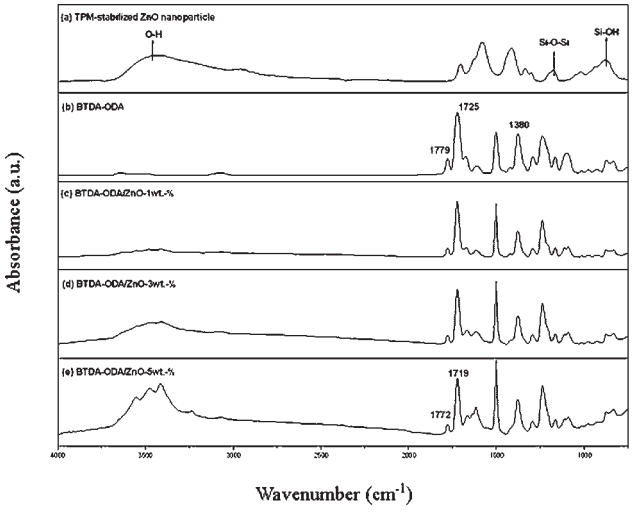

Figure 2. FT-IR spectra of the BTDA-ODA/ZnO hybrid films.

Figure 3 shows the XPS wide-scan spectra of the BTDA-ODA/ZnO-5 wt.-% hybrid film. It shows carbon, oxygen, and zinc characteristic peaks. This confirms that ZnO does appear in the PI hybrid film. But with the different sputtering time needed to detect ZnO at different depths, no Si signal was ever observed in the Si core-level spectra. That is, Si was not able to be detected on the surface and in the bulk of the hybrid film. Two possibilities can account for this: first, the TPM content on the surface of the hybrid films is too low to detect; and/or the surface TPM network decomposes during thermal imidization. In our previous study,[18] the 3-(trimethoxysilyl)propyl methacrylate groups of TPM yield a thin layer of an organic silica nanonetwork capping the ZnO nanoparticles by hydrolysis-condensation reactions.

Figure 4 shows thermogravimetric profiles of the unmodified ZnO nanoparticles and TPM-stabilized ZnO nanoparticles. Both samples show obvious weight loss at temperatures between 300 and 700 °C. This mass loss of the unmodified ZnO nanoparticle is attributed to desorption of acetate anions or acetic acid at the surface of the ZnO nanoparticle.[20] However, TPM-stabilized ZnO nanoparticles shows greater weight loss, 5 wt.-% at 300–700 °C, in comparison with unmodified ZnO nanoparticles. We further analyze the isothermal gravimetric profiles of both

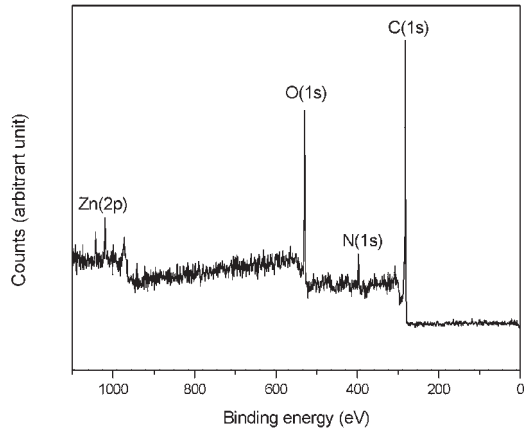

Figure 3. XPS wide-scan spectrum of the BTDA-ODA/ZnO-5 wt.-% hybrid film.

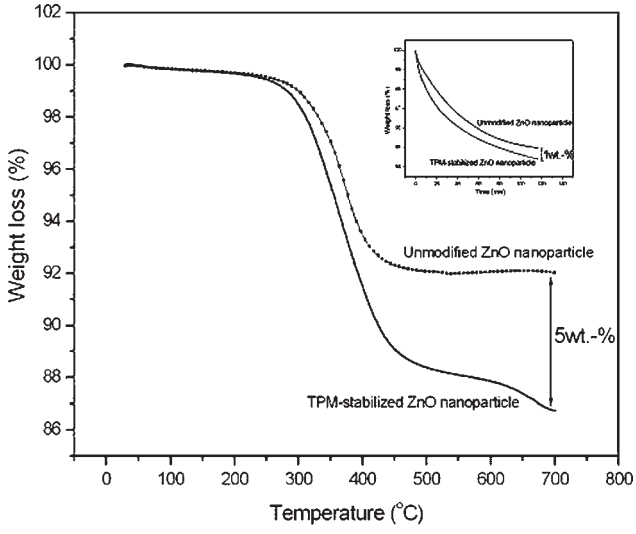

Figure 4. Thermogravimetric profiles of the unmodified ZnO nanoparticle and TPM-stabilized ZnO nanoparticle. The inset shows the thermogravimetric profiles of both samples measured at 300 °C isothermally for 2 h.

samples at 300 °C for 2 h under similar conditions to the imidization. The data reveals that the TPM-stabilized ZnO nanoparticle show a 1 wt.-% larger loss than the unmodified ZnO nanoparticles. Clearly, part of the TPM network (about 20%) decomposes during the imidization at 300 °C for 2 h, but a significant portion of the TPM network stabilizer (about 80%) remains after the imidization.

Figure 5 shows core-level spectra of Zn 2p in the hybrid films with different Zn content. There are two Zn peaks identified; one at 1 019 eV corresponding to Zn 2p3/2, and the other at 1 042 eV is attributed to Zn 2p1/2. The peaks are slightly shifted toward lower energies compared to the spectra of ZnO bulk (1 022 and 1 046 eV corresponds to the Zn 2p2/3 and Zn 2p1/2, respectively).[9] This shift can

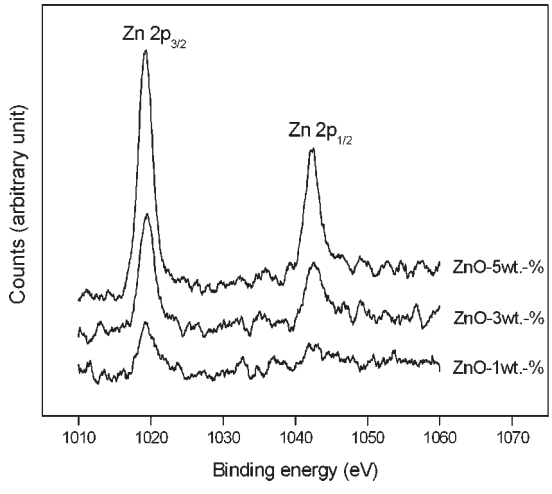

Figure 5. Zn 2p core-level spectra of various BTDA-ODA/ZnO hybrid films with different ZnO content.

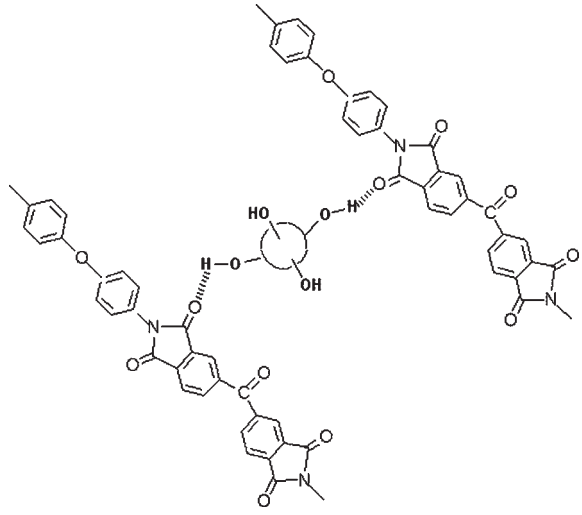

Figure 6. Illustration of the interaction between ZnO nanoparticles and PI.

be attributed to the different chemical environment on the surface of ZnO nanoparticles[5,19] from that of the bulk. In the polymer hybrid, the organic polymer component and the adsorbed organics of low surface energy dominate the surface. This is particularly the case in smaller nanoparticles. This can cause a change in the binding energy of core electrons in Zn atoms.

According to the results of FT-IR spectroscopy, XPS, and TGA, the probable structure of the PI/ZnO nanocomposites can be inferred and is shown in Figure 6. The exposed OH groups on the ZnO nanoparticle surface can bond to the imide group (C=O) of PI through interchain hydrogen bonding to form physical cross-linking. This creates a PI-ZnO interfacial domain with higher T_g.

The coefficient of thermal expansions (CTE) of the PI/ZnO nanohybrid film are listed in Table 1. Both series of the nanohybrid films show the CTE decreasing with increasing ZnO content. In general, the CTEs of the polymer are related to main chain free volume and relaxation.[2] For

Table 1. The coefficient of thermal expansion of pure PI and PI/ZnO nanohybrid films.

ZnO content	BTDA/ODA		PMDA/ODA	
wt.-%	CTE[a)]	CTE decrement	CTE[a)]	CTE decrement
	$ppm \cdot K^{-1}$	%	$ppm \cdot K^{-1}$	%
0	42.5	–	32.5	–
1	40.6	4	25.5	21
3	35.7	16	17.3	47
5	30.8	12	–[b)]	–

[a)] The CTE values are determined from 50 to 250 °C.
[b)] The hybrid film was too brittle to be measured.

our case, ZnO nanoparticles dispersed in the PI matrix reduce the free volume of the molecular structure, and further restrict the segmental relaxation. In addition, the PMDA/ODA hybrid films show a larger CTE decrement than the BTDA/ODA hybrid films. The PMDA/ODA molecular structure is more rigid than BTDA/ODA and has denser molecular packing and less free volume. Even a small amount of 1 wt.-% ZnO nanoparticles doping significantly decreases the CTE of the PMDA-ODA/ZnO hybrid film with a decrement of 21%. The sample with 3 wt.-% of ZnO doping cause a CTE decrement up to 47%. On the other hand, the BTDA/ODA matrix contains a kink point because of the C=O group in the dianhydride fragment. It disturbs chain packing and increases free volume. Hence, the percentage change in CTE in this series of hybrid film is much less than that of the corresponding PMDA-ODA/ZnO hybrid film.

The dynamic mechanical analyses of PI/ZnO hybrid films are shown in Figure 7 and 8. In Figure 7, the storage moduli of both PMDA-ODA/ZnO and BTDA-ODA/ZnO nanohybrid films increase with increasing ZnO content. In addition, all the hybrid films have a larger storage modulus than pure PI in the test temperature range. The tan δ curves of the all samples are shown in Figure 8. With increasing ZnO content, both series of hybrid films show higher transition temperatures and lower damping in comparison with the pure PI. This is attributed to the physical cross-linking through hydrogen bonding in the PI/ZnO hybrid film as shown in Figure 6. In addition, the series of BTDA/ODA hybrid films show the tendency of two damping peaks (Figure 8a) with increasing ZnO content. This phenomenon can be further analyzed by deconvolution of tan δ curves and the results are shown in Figure 9 and listed in Table 2. The tan δ curve of BTDA-ODA/ZnO nanohybrid films can be resolved into two curves, tan δ_1 with T_{g1} and tan δ_2 withT_{g2}. Both T_{g1} and T_{g2} shift to higher temperature with increasing ZnO content, and tan δ_1 damping decreases as well as tan δ_2 increases with increasing ZnO content. As in our previous report om PI/TiO_2 hybrid films,[6] the peaks of tan δ_1 and tan δ_2 are related to the pure PI matrix and the PI/inorganic interfacial domains, respectively. The virgin PMDA/ODA PI film is more rigid than the BTDA/ODA film

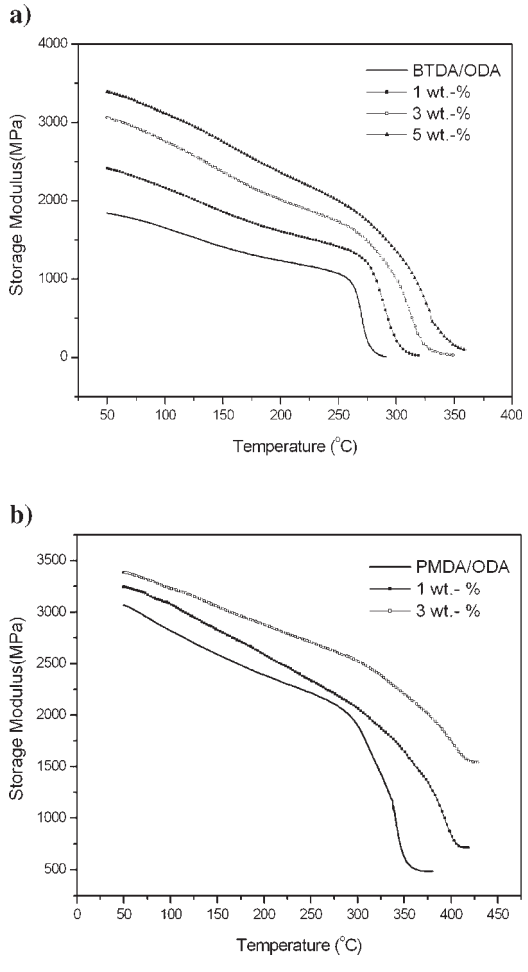

Figure 7. Dynamic mechanical storage moduli of (a) BTDA-ODA/ZnO, and (b) PMDA-ODA/ZnO hybrid films.

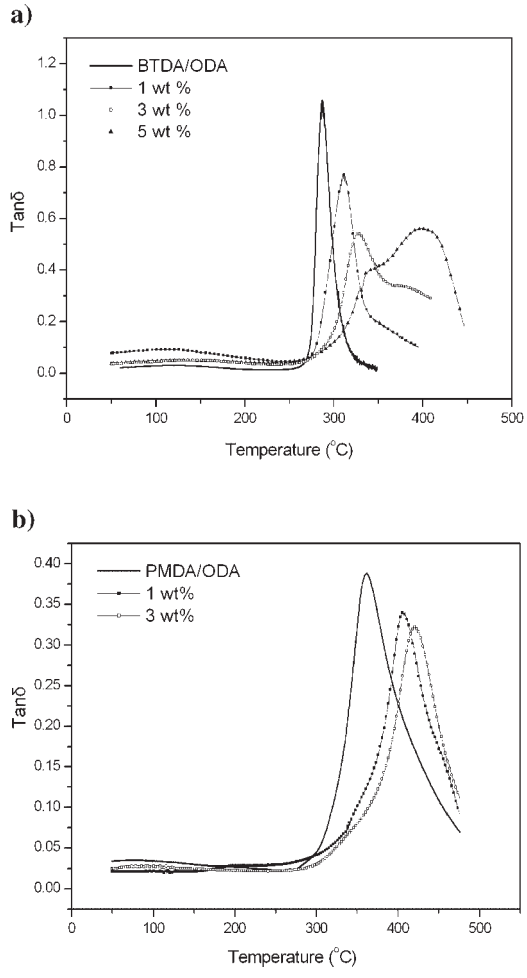

Figure 8. Dynamic mechanical tan δ curves of the PI/ZnO hybrid films: (a) BTDA-ODA/ZnO, and (b) PMDA-ODA/ZnO.

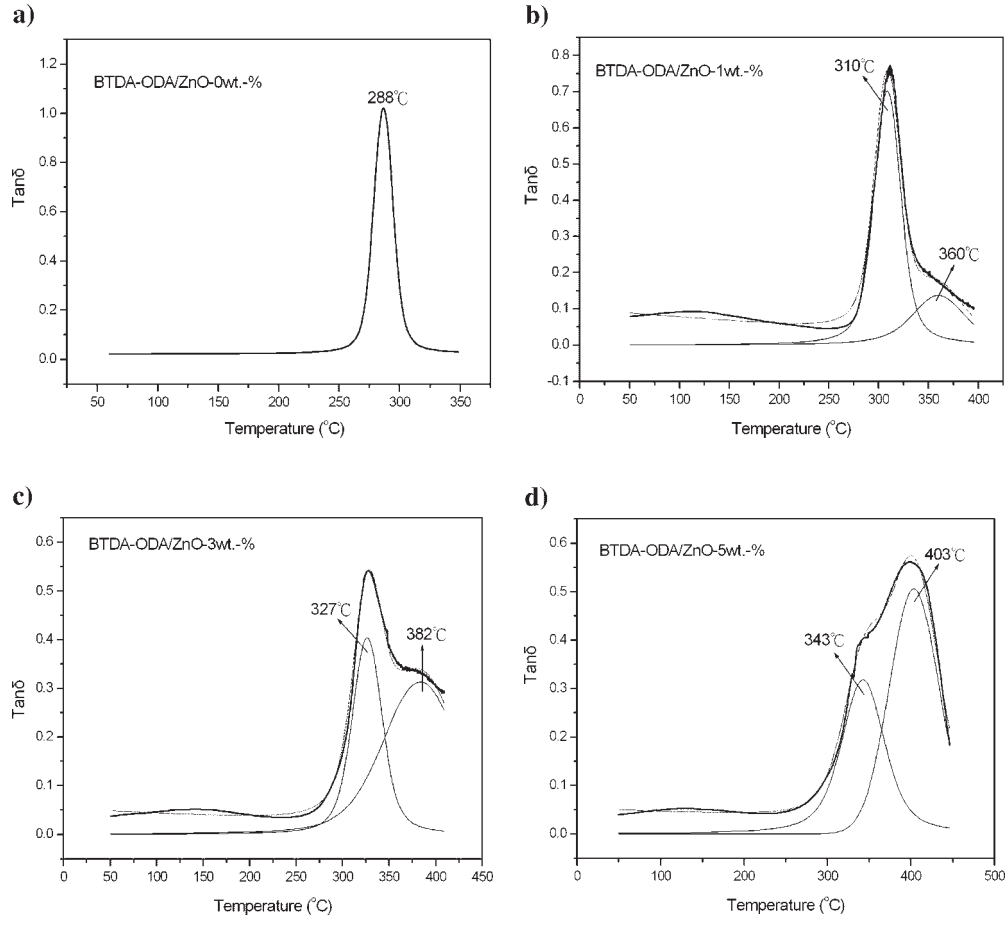

Figure 9. Deconvolution of tan δ curves of BTDA-ODA/ZnO nanohybrid films.

and has a higher T_g. It gives the chance for the two tan δ peaks to overlap into one peak in the rigid PI/ZnO nanohybrid. Therefore, the series of PMDA/ODA hybrid films show only one tan δ in Figure 8b.

Figure 10(a) shows the thermogravimetric profiles of the BTDA-ODA/ZnO nanohybrid films. The T_d decreases with increasing ZnO content, and shifts from 579 (pure BTDA/ODA) to 484 °C (5 wt.-% ZnO). The dramatic decrease in thermal stability of the hybrid films can be attributed to two reasons: metallic-compound-induced oxidation, which can oxidatively degrade PI films;[5] and the desorption of the organic molecules, which are adsorbed at the ZnO nanoparticles surfaces.[20] As shown in Figure 10(b), the PMDA-ODA/ZnO nanohybrid films show a similar phenomenon, but the T_d decrement is less significant, as shown in Table 3. It seems that the rigid PMDA-ODA is more resistant to the ZnO oxidative degradation.

Table 2. Glass transition temperatures (T_g's) of pure PI and PI/ZnO nanohybrid films determined by DMA measurement.

ZnO content	1st Transition				2nd Transition	
wt.-%	BTDA/ODA		PMDA/ODA		BTDA/ODA	
	T_{g1}	ΔT_{g1} [a]	T_{g1}	ΔT_{g1}	T_g	ΔT_g [b]
	°C	°C	°C	°C	°C	°C
0	288	–	362	–	–	–
1	310	+22	405	+43	360	+50
3	327	+39	420	+58	382	+55
5	343	+55	–[c]	–	403	+60

[a] $\Delta T_{g1} = T_{g1}$ of hybrid film $- T_{g1}$ of pure PI.
[b] $\Delta T_g = T_{g2} - T_{g1}$.
[c] The hybrid film was too brittle to be measured.

TEM images of TPM-stabilized ZnO nanoparticle, BTDA-ODA/ZnO-5 wt.-%, and PMDA-ODA/ZnO-5 wt.-% hybrid films are shown in Figure 11. The as-synthesized TPM-stabilized ZnO nanoparticle are spheres with a particle size of 3–4 nm (Figure 11a). In Figure 11(b), the ZnO particles are of a uniform dispersion in the BTDA/ODA matrix, but the nanoparticles are bigger (10–15 nm) than the as-synthesized particles. Some are elongated. The change in size and shape can be attributed to the high temperature and long time of the imidization process. During the period of the thermal treatment, the silica network caps are partially decomposed and released from the surface of the ZnO nanoparticles. The less-protected particles can undergo crystal growth individually or can aggregation with

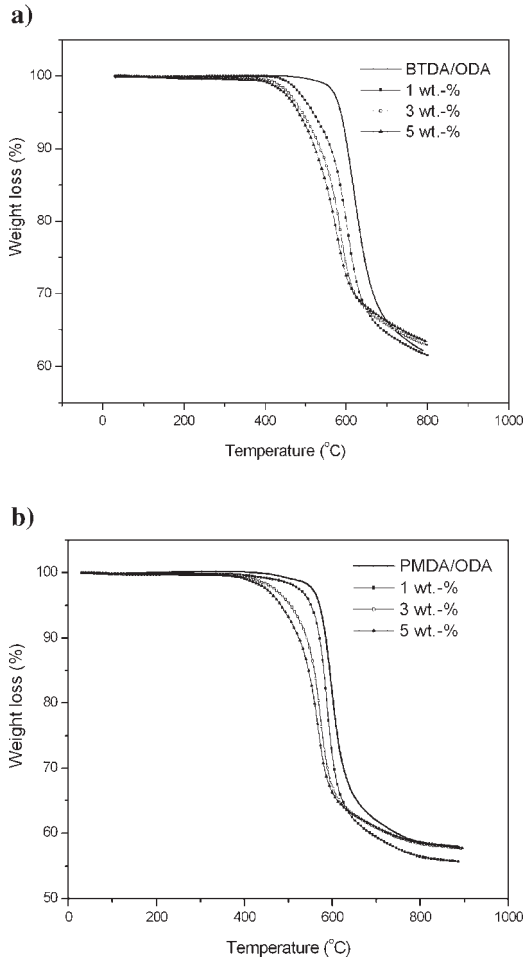

Figure 10. Dynamic thermogravimetric profiles of (a) BTDA-ODA/ZnO and (b) PMDA-ODA/ZnO nanohybrid films.

another growing particle resulting in change of particle size and shape.[18,20] The ZnO particles show notable aggregation as well as irregular shape in the PMDA/ODA matrix, and the average particle size (30–40 nm) is much larger than the ZnO nanoparticles in the BTDA-ODA/ZnO hybrid film. The rigid structure of the PMDA-ODA causes ZnO

Table 3. Thermogravimetric analysis of pure PI and PI/ZnO nanohybrid films.

ZnO content	BTDA/ODA		PMDA/ODA	
wt.-%	T_d[a)]	T_d decrement	T_d	T_d decrement
	°C	°C	°C	°C
0	579	–	575	–
1	520	59	553	22
3	491	88	505	70
5	484	95	487	88

[a)] 5 wt.-% decomposition temperature measured under N_2.

Figure 11. TEM images of (a) TPM-stabilized ZnO nanoparticles, (b) BTDA-ODA/ZnO-5 wt.-%, and (c) PMDA-ODA/ZnO-5 wt.-% hybrid films.

nanoparticle aggregation and crystal growth more readily than in BTDA-ODA, which has a kink structure and is more flexible.

Conclusion

The data from FT-IR spectroscopy, XPS, TGA, and DMA analyses infer that the morphology of PI/ZnO nanohybrid films arises from interchain hydrogen bonding between the ZnO nanoparticles and the PI matrix. The interchain hydrogen bonding, being a kind of physical cross-linking, exists in the PI-ZnO interfacial domain. Owing to this physical cross-linking, the storage modulus, CTE decrement, and T_g of the hybrid films can be effectively improved in comparison with that of pure PI. The improvements on these characteristics of PMDA-ODA/ZnO nanohybrid films are much more significant than that of BTDA-ODA/ZnO nanohybrid films. The physical cross-linking structure also causes BTDA-ODA/ZnO nanohybrid films to have two T_g's, one for the pure PI domain, the other higher T_g for the the PI-ZnO interfacial domain. PMDA-ODA/ZnO nanohybrid films have only one T_g because the PMDA-ODA, having a high T_g results in the two T_g's to overlap and become one. Although the T_d of the hybrid films are lower than for pure PI, it is good enough for practical application. From TEM images, the ZnO particles show a uniform dispersion in the BTDA/ODA matrix, but most particles are bigger in size (10–15 nm) and some are elongated in comparison with the as-synthesized TPM-stabilized ZnO nanoparticles. This can be attributed to the high temperature and long time taken for the imidization process. However, the aggregation, as well as irregular shape, of the ZnO nanoparticles are more notable in the PMDA-ODA/ZnO hybrid film. The matrix structures significantly affect the morphology and characteristics of the PI/ZnO nanohybrid films.

Acknowledgements: The authors gratefully acknowledge the *National Science Council of the Republic of China* NSC 92-2216-E-009-003 and the *Lee and MTI Center* in NCTU for financial support of this work.

[1] K. Akamatsu, S. Ikeda, *Chem. Mater.* **2003**, *15*, 2488.
[2] C. T. Yen, W. C. Chen, *Polymer* **2003**, *44*, 7079.
[3] C. C. Chain, W. C. Chen, *Chem. Mater.* **2002**, *14*, 4242.
[4] L. Li, L. Qinghua, *Mater. Sci. Eng.* **2002**, *22*, 61.
[5] P. C. Chiang, W. T. Whang, *Polymer* **2003**, *44*, 2249.
[6] P. C. Chiang, W. T. Whang, *Thin Solid Film* **2003**, *447*, 359.
[7] P. C. Chiang, W. T. Whang, *Polymer* **2004**, *45*, 4465.
[8] C. H. Hung, W. T. Whang, *Mater. Chem. Phys.* **2003**, *82*, 705.
[9] N. S. Pesika, Z. Hu, *J. Phys. Chem. B* **2002**, *106*, 6985.
[10] L. Spanhel, M. A. Anderson, *J. Am. Chem. Soc.* **1991**, *113*, 2826.
[11] L. Guo, S. Yang, *Chem. Mater.* **2000**, *12*, 2268.
[12] E. M. Wang, P. G. Hoertz, *Langmuir* **2001**, *17*, 8362.
[13] C. G. Kim, K. Sung, *Chem. Commun.* **2003**, *16*, 2068.
[14] M. Abdullah, T. Morimoto, *Adv. Funct. Mater.* **2003**, *13*, 800.
[15] J. I. Hong, L. S. Schadler, *Appl. Phys. Lett.* **2003**, *82*, 1956.
[16] H. M. Xiong, X. Zhao, *J. Phys. Chem. B* **2001**, *105*, 10169.
[17] J. Zheng, R. W. Siegel, *J. Polym. Sci., Part B: Polym. Phys.* **2003**, *41*, 1033.
[18] C. H. Hung, W. T. Whang, *J. Mater. Chem.*, in press.
[19] L. J. Meng, C. P. Moreira, *Appl. Surf. Sci.* **1994**, *78*, 57.
[20] V. Noack, *Chem. Mater.* **2002**, *14*, 1411.
[21] H. B. Park, J. K. Kim, *J. Membr. Sci.* **2003**, *220*, 59.

